emission from the surface, and (c) at high concentration the hardening is developed by strong trapping and local hydride formation.

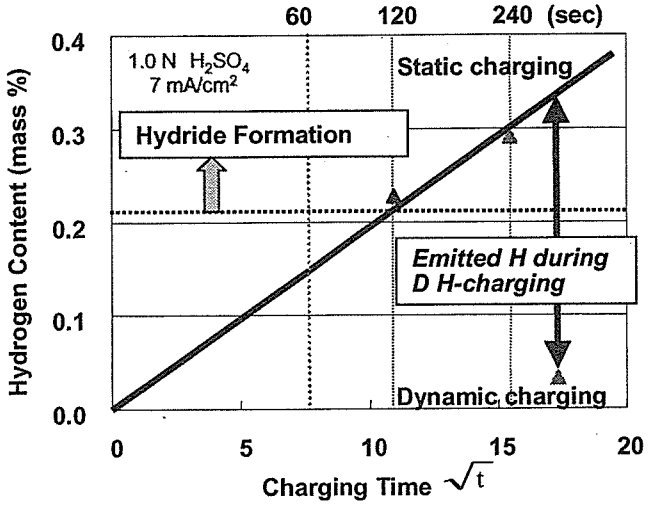

FIGURE 7. Hydrogen content as the function of static and dynamic charging time. The content increases with static charging time, but is significantly lower for dynamic charging.

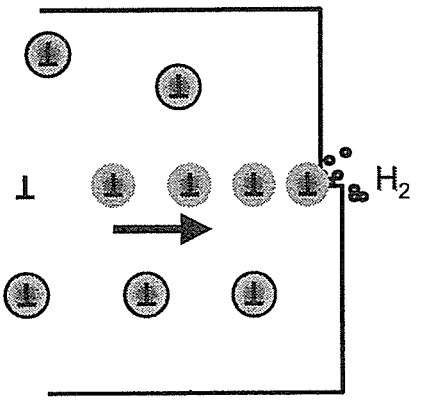

FIGURE 8. A schematic diagram of the dynamic interaction between H dislocations for the softening, hardening and gas emission; a) dislocation mobility is enhanced by the hydrogen atmosphere, b) the dislocation gliding with H trapping produces gas emission, and (c) strong trapping and local hydride formation produce hardening.

CONCLUSION

To clarify the hydrogen behavior under the deformation of vanadium and vanadium alloys, static and dynamic chargings were carried out for both V and V-4Cr-4Ti, where a part of sample was neutron-irradiated. The desorption profile showed that hydrogen can be trapped by lattice defects; dislocations, vacancies and voids, and was relatively stable up to 500 C. In case of un-irradiated materials, the unexpected softening occurred at low hydrogen levels, and hardening developed at high levels. The hydrogen-induced softening and hardening seems to be general phenomena in V and its alloys. A significant effect was observed during dynamic charging experiment, which was attributed to fast diffusion and interactions with mobile dislocations. The

results suggest that hydrogen-induced phenomena can be attributed to high hydrogen diffusivity under deformation and the enhanced movement of dislocations, as well as dislocation capture from hydride formation at high hydrogen concentrations.

ACKNOWLEDGMENTS

Authors will express thanks Prof. T. Muroga and T. Nagasaka of National Institute of Fusion Science for high quality specimens.

REFERENCES

1. G. Alefeld, J. Völkl, Hydrogen in Metals, 1978, pp. 332-333.
2. J. Chen, S. Qiu, J. Nucl. Mater, **302**, 135-142 (2002).
3. . R. Greenwood, B. M. Oliver, S. Ohnuki, K. Shiba, Y. Kohno, A. Kohyama, J. P. Robertson and D. S. Gelles, J. Nucl. Mater. **283-287**, 1438-1442 (2000).
4. S. Ohnuki, H. Takahashi and F. A. Garner, ASTM STP1366, M. L. Hamilton, A. S. Kumar, S. T. Rosinski, and M. L. Grossbeck, Eds., ASTM (2000) pp.1212-1225.
5. T. Nagasaka et. al, Low Activation Characteristic of Several Heats of V-4Cr-4Ti Ingots, NIFS report, (2002).
6. P. E. Torres, K. Aoyagi, T. Suda, S. Watanabe, S. Ohnuki: Hydride Formation and Mechanical Properties in Vanadium Alloys, J. of Nucl. Mater., **307-311**, 625-629 (2002).
7. K. Aoyagi, P. E. Torres, T. Suda, S. Watanabe and S. Ohnuki, Effect of Hydrogen Accumulation on Mechanical Property and Microstructure in V-Cr-Ti Alloys, J. Nucl. Mater. **283-287**, 876-879 (2000).
8. M. Kanedome, Y. Wang, T. Yasuda, T. Suda, S. Watanabe, S. Ohnuki, T. Nagasaka, T. Muroga, Dynamic and Static Hydrogen Effects on the Mechanical Properties in Vanadium, J. Nucl. Mater., to be published.
9. T. Yasuda, Master Thesis, Hokkaido University, (2006), to be published.

Korean J. Electron Microscopy Special Issue 1, 57~61(2006)

In-situ Observation of Hydride Stability of Vanadium Alloys in Electron Microscope

S. Ohnuki*, K. Takase, K. Yashiki, K. Hamada, T. Suda and S. Watanabe
Division of Materials Science, Graduate School of Engineering,
Hokkaido University, Sapporo, 060-8278, Japan
(Received July 19, 2005; Accepted March 24, 2006)

ABSTRACT

High-resolution microscopy was applied for surveying hydride stability in Vanadium alloys, which are candidate for hydrogen storage materials of advanced hydrogen energy systems. V_2H hydride in V alloys was stable at room temperature under the vacuum condition, but it was decomposed during heating up to 100°C. It was confirmed from HRTEM image and FFT that V_2H has a BCT structure, where hydrogen atoms locate at octahedral sites. Crystal orientation was $<110>$beta//$<110>$mat., and lattice strain is about 10%. After the decomposition of the hydride, relatively large lattice expansion was observed in the matrix, which suggests that hydrogen atoms should be trapped by lattice defects and included in the matrix. Intensive electron beam also enhanced the decomposition.

Key words : FFT, HRTEM, Hydride stability

INTRODUCTION

V-Cr-Ti alloys with body centered cubic structure have a potential for using practical hydrogen-storage alloys, because of high hydrogen storage capacity (Cho et al., 1999; Okada et al., 2002; Tamura et al., 2003). However, the hydrogen capacity strongly depends on the composition and fabrication methods, which means that lattice defects can influence the hydrogen behavior, as well as solute atoms. In V-Cr-Ti alloys we know two types of hydrides; VH_2 and V_2H (Reilly & Wiswall, 1970; Fujita et al., 1979), depending on hydrogen concentration and temperature. The former is main compound for hydrogen storage behavior, but the later is the hydride can be formed at low hydrogen pressure side and relatively stable. Mechanisms of absorption and desorption are also impotent.

Materials issues of V-Cr-Ti alloys for increasing hydrogen storage capacity are to reducing solubility limit and decreasing remained hydride, which means that the stability of hydrides are important. From these reason, high resolution electron microscopy (HRTEM) and "in-situ" observation were carried out to clarify the structure of hydride and interface as well as hydride stability.

MATERIALS AND METHODS

High purity vanadium sample was provided from National Institute of Fusion Science. The sample has full-annealed structure due to final heat-treatment at 1,100°C. Hydrogenation was carried out for 3 mm disks under 0.1 MPa of H_2 gas condition at 400°C to RT, where nominal content of hydrogen was estimated to be about 1 at%. TEM samples were electro-polished by conventional twin-jet method in H_2SO_4+ethanol solution.

For high resolution microscopy, we used VEM of 1.25 MeV installed at Hokkaido University. Furies function transfer (FFT), inverse Furies function transfer (IFFT) and Mac TEMPUS were used for structural an-

* Correspondence should be addressed to Dr. S. Ohnuki, Division of Materials Science, Graduate School of Engineering, Hokkaido University, Sapporo, 060-8278, Japan.

alysis and calculation of diffraction and images. In-situ heating experiment was carried out in the HVEM to clarify the hydride stability up to 100°C, where a digital video system used for recording images. After video-capture we applied FFT and IFFT to get detailed data on plane distance and rotation.

RESULTS AND DISCUSSION

1. Structural analysis of hydride

Fig. 1 shows HREM, FFT and IFFT images from typical area including both of V matrix and a hydride precipitate (PPT) which locates at edge-on condition. The lattice planes with about 1 nm extend to <110> direction, which means <110>beta//<110>mat. But the interface between PPT and matrix was distorted, which direction is parallel to <110> in the matrix.

Fig. 2 shows a simple crystal model for beta-hydride (V_2H) of bct structure, one of which is (010) view and other is (100) view, where lattice was expanded by 10% along to c-axis for simulating the structure. Large balls are V atom and small ones are hydrogen atoms which locate at octa-headral sites, where the total structure is an ordered phase. By using the crystal model, we calculated diffraction pattern as shown in Fig. 1. It is well

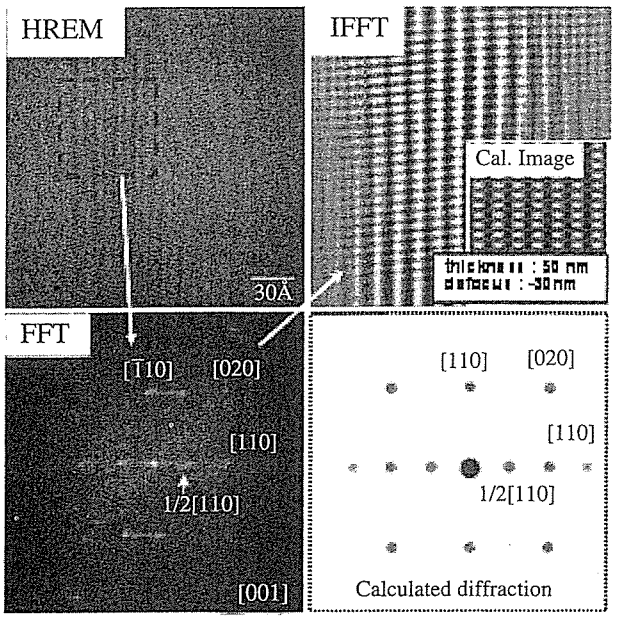

Fig. 1. High resolution image of hydride precipitate (V_2H) and calculated image from simple crystal; model.

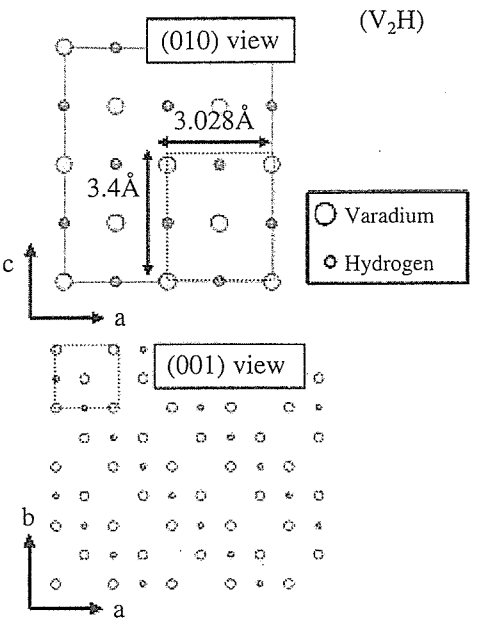

Fig. 2. Simple crystal model embedded hydrogen atoms in BCT structure.

consisted with FFT from actual PPT in basically, for example, 1/2 (110) spots are reproduced by the calculated pattern. But, comparing in the detail, we could realize some distortion occurred in the actual PPT, see FFT in Fig. 1.

Fig. 3 shows the interface structure between bcc matrix and hydride. By using FFT/IFFT, we can confirm that the structure contains large amount of strain along <110> directions. The incoherent interface should include plain defects and dislocations, which were observed in the photographs. Fig. 4 shows the model of diffraction spots from V matrix (white circles) and hydride precipitate (dark circles). The crystallographic relation is not ideal, and the distortion occurred in diffraction pattern are more than in the model, which showing un-isotropic strain.

2. Macroscopic in-situ observation

No structural change of the hydride was observed in a vacuum condition of the microscope at RT. Fig. 5 shows the continuous observation of hydride structure under intensive electron beam: 1.25 MeV HVEM at RT, where the hydride was decomposed during e-irradiation. The decomposition was so quick within 80 sec, which means it may be an irradiation-enhanced process. After

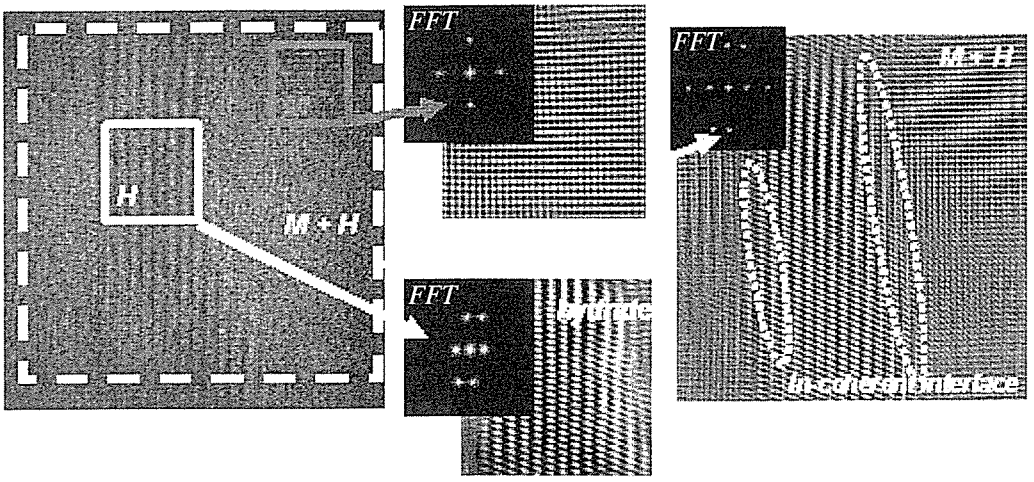

Fig. 3. Lattice image, FFT and IFFT from hydride and matrix. Large distortion can be observed at the interface.

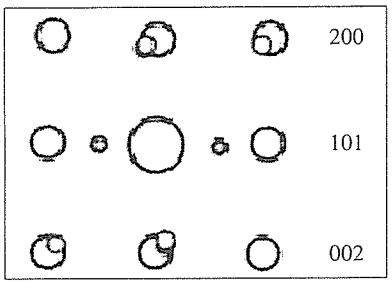

Fig. 4. SADP of $<100>$ from hydride and matrix, which is showing the rotation to $<110>$.

the decomposition, defect clusters (dislocation loops) were developed, which suggested many factors, for example, H trapping by defect clusters, high energy particle collision, dissolution and enhanced-diffusion.

3. Hydride decomposition

Fig. 6 shows in-situ observation of hydride decomposition during heating at 100°C, where the high resolution electron microscopy (HREM) was carried out from the direction of $<111>$. They were recorded in digital VTR system. Images are composed of wide and narrow lattices, but distorted partially which consist with the local strain. FFT which equivalent with selected area diffraction pattern indicates this area is beta-hydride of bct structure. With heating the decomposition progressed quickly, and the structure turned to bcc within 2 min, as shown in FFT. However, some lattice defects remained in the bcc structure, as shown in the circle, which is assumed to be dislocations.

Fig. 7 shows the sets of lattice images from FFT and

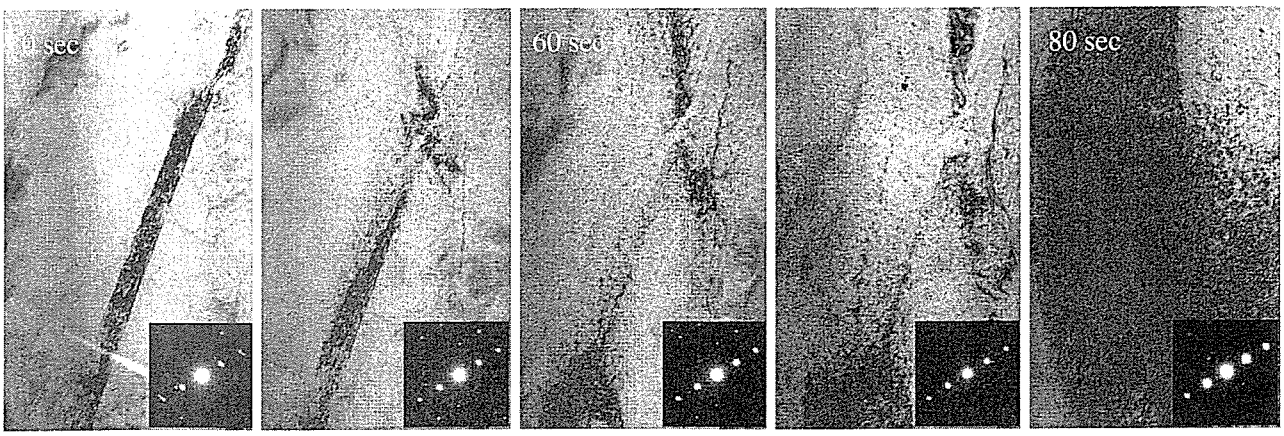

Fig. 5. disappearing hydride and developing radiation damage during observation with intensive beam at room temperature.

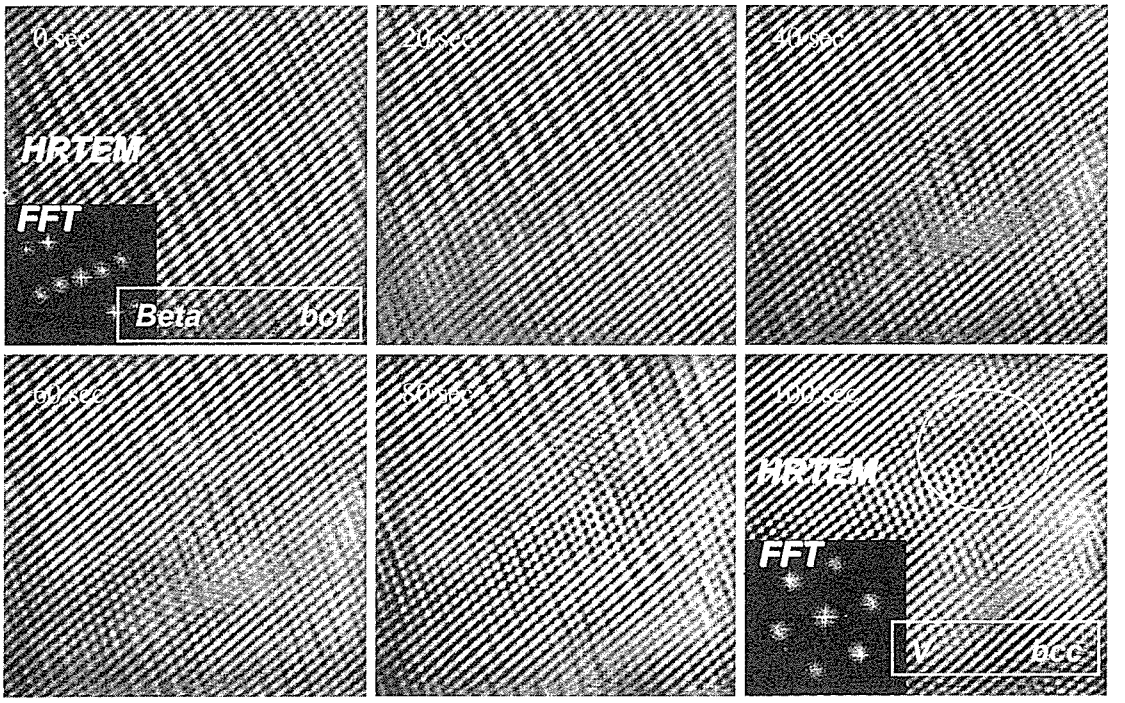

Fig. 6. Lattice image and FFT during heating observation at 100°C. The hydride of V_2H was decomposed and return to BCC lattice up to 100 sec.

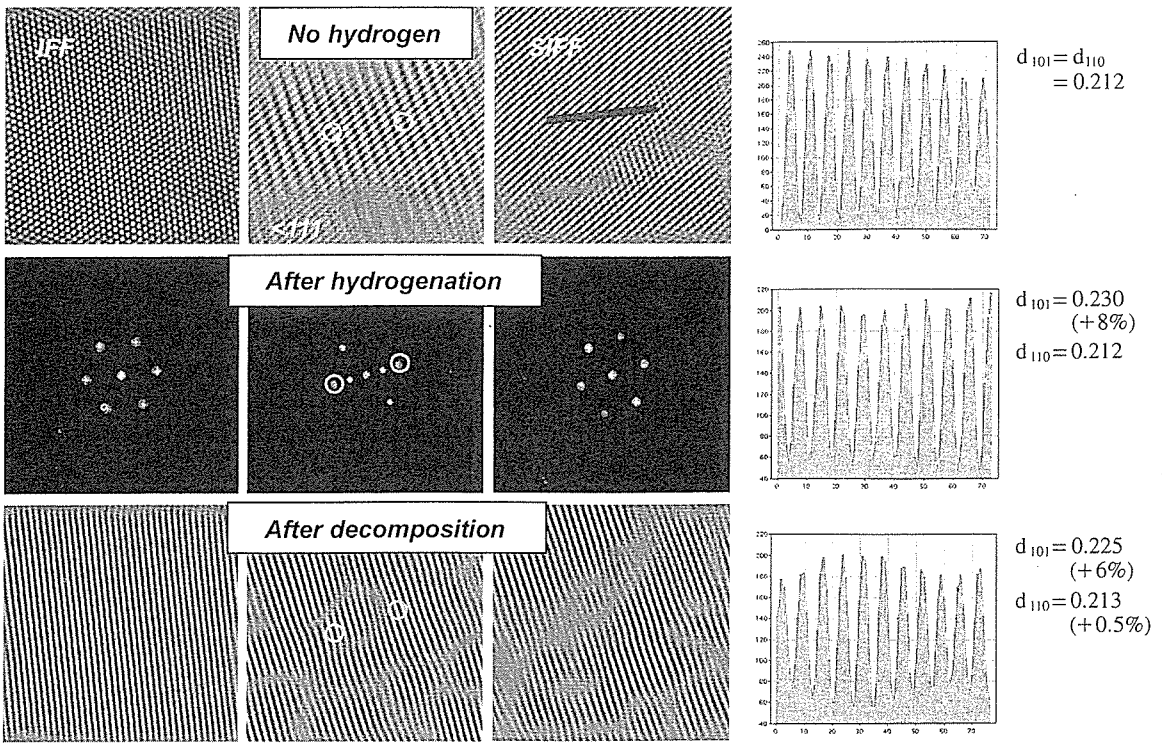

Fig. 7. Lattice image, local diffraction and selected lattice image from IFF, FFT and SIFFT. Mean lattice plane distance was estimated from SIFFT images.

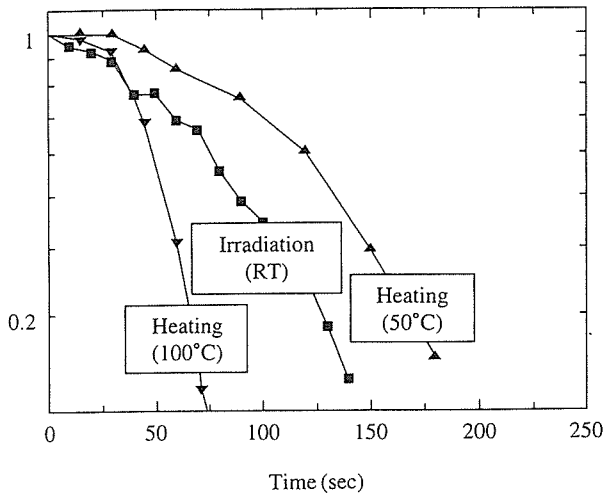

Fig. 8. Relative intensity of V_2H as a function of observation time at different temperature.

IFFT of the typical lattice plane in hydride area annealed at 50°C. We confirmed reproducibility for this hydride decomposition at the temperature range. The diffraction pattern from FFT shows the transition of bcc-bct-bcc, where the zone axis is $<111>$. A pair of {110} diffraction spots were selected for estimating plane distance. In the uncharged V sample, the plane distance of three pair of {110} was 0.212 nm, which means it is isotropic structure. In the H-charged specimen, the plane distance of (101) was 0.230 nm, but other sets of planes did not change, which means the hydride produced expanding unisotropic to [101] direction with +8%. After decomposition, FFT spots basically returned to bcc structure, but we observed some defective parts, and the plane distance of (101) was 0.225 nm, and the distance of (110) was 0.213 nm. It should be noted that V matrix remains the strain of +5% after H decomposition, which means that bcc lattice strained in solid solution at this temperature. It can be suggested some kind of H-trapping should be existed in solution condition.

Fig. 8 shows the changing of hydride fraction as a function of observation time. Beta hydride can be decomposed by heating within several minutes. In the case of intensive electron beam, the decomposition was enhanced, so it is a radiation-enhanced process.

CONCLUSIONS

The thermal stability of hydride in Vanadium has been studied by means of high resolution electron microscopy and in-situ heating experiment. Hydride (V_2H) is relatively stable at room temperature in vacuum condition. Hydride is decomposed during heating up to 100°C. In the structure of V_2H, hydrogen locates periodically at octa-headral sites, and shows bct structure with extending c-axis. Crystal orientation is basically $<110>$beta//$<110>$mat. Interface between hydride and matrix is in-coherent with large lattice strain of over 10%. Even after hydride decomposition, lattice expansion remains; this is due to dissolved hydrogen. Intensive electron beam enhances the decomposition, which means an irradiation-enhanced process.

REFERENCES

Cho SW, Han CS, Park CN, Akiba E: J Alloys Comp 288 : 294-298, 1999.

Fujita K, Huang YC, Tada M: J Jpn Inst Met 43 : 601-609, 1979.

Okada M, Kuriiwa T, Tamura T, Takamura H, Kamegawa A: J Alloys Comp 330-332 : 511-516, 2002.

Reilly JJ, Wiswall RH: Inorg Chem 9 : 1678-1682, 1970.

Tamura T, Kazumi T, Kamegawa A, Takamura H, Okada M: J Alloys Comp 356-357 : 505-509, 2003.

Hydrogen Absorption of Titanium and Nickel-Titanium Alloys During Long-Term Immersion in Neutral Fluoride Solution

Ken'ichi Yokoyama,[1] Toshio Ogawa,[2] Kenzo Asaoka,[1] Jun'ichi Sakai[2]

[1] Department of Biomaterials and Bioengineering, Institute of Health Biosciences, The University of Tokushima Graduate School, 3-18-15 Kuramoto-cho, Tokushima 770-8504, Japan

[2] Department of Materials Science and Engineering, Waseda University, 3-4-1 Okubo, Shinjuku-ku, Tokyo 169-8555, Japan

Received 13 January 2005; revised 6 September 2005; accepted 8 September 2005
Published online 16 December 2005 in Wiley InterScience (www.interscience.wiley.com). DOI: 10.1002/jbm.b.30485

Abstract: Hydrogen absorption of biomedical titanium and Ni-Ti alloys in a neutral fluoride (2.0% NaF) solution for up to 10,000 h at 37°C has been evaluated by means of hydrogen thermal desorption analysis. For α titanium (commercial pure titanium), the amount of absorbed hydrogen was, at most, 10–30 mass ppm, and the corrosion product and hydride formation were revealed on the surface of the specimen by X-ray diffraction analysis. Ni-Ti superelastic alloy absorbed ~150 mass ppm of hydrogen, which was probably sufficient to result in the pronounced degradation of the mechanical properties, although corrosion was hardly observed. In contrast, hydrogen absorption of α-β titanium (Ti-6Al-4V) and β titanium (Ti-11.3Mo-6.6Zr-4.3Sn) alloys was negligible, although general corrosion was observed. The results of the present study indicate that the susceptibility of titanium and Ni-Ti alloys to hydrogen absorption in the neutral fluoride solution is different from that in the acidic fluoride solution reported previously. © 2005 Wiley Periodicals, Inc. J Biomed Mater Res Part B: Appl Biomater 78B: 204–210, 2006

Keywords: titanium; Ni-Ti alloy; hydrogen embrittlement; corrosion; fluoride

INTRODUCTION

Hydrogen embrittlement of titanium and Ni-Ti alloys with mainly titanium oxide film, which are used widely in biomedical applications such as dental implants and orthodontic wires, occasionally occurs in the oral cavity. One reason for hydrogen embrittlement in the oral cavity is contact with fluoride present in prophylactic agents or toothpastes.[1–7] In acidic fluoride solutions, titanium and Ni-Ti alloys are prone to corrosion even though the contact is for a short-term.[8–14] During corrosion in acidic fluoride solutions, titanium and Ni-Ti alloys absorb sufficient amounts of hydrogen to cause degradation of the mechanical properties or fracture. The characteristics of hydrogen embrittlement of titanium and Ni-Ti alloys in acidic fluoride solutions have been detailed in our previous articles.[1–7]

In neutral fluoride solutions, hydrogen embrittlement of titanium and Ni-Ti alloys has not yet been clarified. From the results of electrochemical experiments for short-term immersion, the corrosion and the degradation of the mechanical properties of titanium and Ni-Ti alloys rarely occurred in neutral fluoride solutions. However, under a sustained tensile-loading test in neutral fluoride solutions lasting up to 1000 h at room temperature, α titanium (commercial pure titanium)[3] and Ni-Ti superelastic alloy[4] fracture, suggesting that hydrogen absorption occurs. The α-β titanium[7] and β titanium alloys[2] do not fracture, although they do undergo general corrosion during the sustained tensile-loading test. The corrosion possibly leads to hydrogen absorption. Therefore, it is necessary to confirm experimentally whether hydrogen absorption of titanium and Ni-Ti alloys takes place in neutral fluoride solutions during long-term immersion, that is, longer than 1000 h.

The purpose of this study is to evaluate hydrogen absorption of biomedical titanium and Ni-Ti alloys during long-term immersion in neutral fluoride solution using hydrogen thermal desorption analysis (TDA). From the viewpoint of fundamental study on hydrogen absorption, immersion tests were performed without applied stress lasting up to 10,000 h.

EXPERIMENTAL PROCEDURES

The 0.50-mm wires of α titanium (commercial pure titanium), the α-β titanium alloy (Ti-6Al-4V alloy), the Ni-Ti superelastic alloy, and 0.45-mm wires of the β titanium alloy (TMA; Ormco Corporation, Glendora, CA) were cut into

Correspondence to: K. Yokoyama (e-mail: yokken@dent.tokushima-u.ac.jp)
Contract grant sponsor: Ministry of Education, Culture, Sports, Science and Technology, Japan; contract grant numbers: 14771090 and 15560632

TABLE I. Chemical Compositions of Tested Specimens (mass %)

	Ti	C	H	O	N	Fe	Al	V	Mo	Zr	Sn	Ni
α Titanium	Balance	0.003	0.0010	0.107	0.003	0.026	–	–	–	–	–	–
α-β Titanium alloy	Balance	0.01	0.0011	0.18	0.01	0.22	6.22	4.1	–	–	–	–
β Titanium alloy	77.8	–	–	–	–	–	–	–	11.3	6.6	4.3	–
Ni-Ti superelastic alloy	Balance	–	–	–	–	–	–	–	–	–	–	55

specimens of 50 mm long. The nominal chemical compositions of these wires are given in Table I. Percent in this article means mass percent, unless otherwise stated. The specimens were carefully polished with 600-grit SiC paper and ultrasonically washed in acetone for 5 min. The specimens were immersed separately in 50 mL of aqueous solution of 2.0% NaF of pH 6.5 at 37°C for up to 10,000 h. For Ni-Ti superelastic alloy, the volume of the test solution was 10 mL for comparison with our previous study.[1]

The corrosion potential of the specimens was measured at 37°C in 2.0% NaF solution under aerated conditions. The counter and reference electrodes used were a platinum electrode and a saturated calomel electrode (SCE), respectively. The measurements were started 10 s after immersion in the test solutions.

The amount of desorbed hydrogen was measured by TDA for the immersed specimens (n = 1 or 2). The immersed specimens were cut at both ends and subjected to ultrasonic cleaning with acetone for 2 min. Subsequently, the specimens were dried in ambient air and then measured. TDA was started 30 min after the removal of specimens from the test solution. A quadrupole mass spectrometer (ULVAC, Kanagawa, Japan) was used for hydrogen detection. Sampling was conducted at 30 s intervals at a heating rate of 100°C/h.

The side surface of the immersed specimens was observed by scanning electron microscopy (SEM). The corrosion products on the surface of the immersed specimens and the surfaces after removal of the corrosion products were examined by X-ray diffraction (XRD) analysis with Cu Kα radiation of wavelength λ = 1.54056 Å in the 2θ angle range from 10° to 90° operated at 40 kV and 30 mA.

EXPERIMENTAL RESULTS

Changes in corrosion potentials in the 2.0% NaF solution under aerated conditions for the short term are shown in Figure 1. The potentials of the α-β titanium, β titanium, and Ni-Ti superelastic alloys were stabilized between −0.3 and −0.4 V (vs. SCE), whereas the final potential of α titanium was −0.6 V (vs. SCE).

The total amounts of hydrogen desorbed from specimens immersed in 2.0% NaF solution are shown as functions of immersion time in Figure 2. The amount of hydrogen absorbed during the immersion test can be calculated by subtracting the amount of hydrogen desorbed from a nonimmersed specimen, that is, predissolved hydrogen content, from the total amount of desorbed hydrogen. The predissolved hydrogen contents of α titanium, and the α-β titanium, β titanium, and Ni-Ti superelastic alloys were approximately 42, 96, 140, and 7 mass ppm, respectively. The amount of absorbed hydrogen in the Ni-Ti superelastic alloy was ~150 mass ppm, although hydrogen absorption was almost saturated after 2000 h. For α titanium, the amount of absorbed hydrogen was at most 10–30 mass ppm. In contrast, increments in the amount of desorbed hydrogen of the α-β titanium and β titanium alloys were hardly detectable. After 10,000 h, the amounts of desorbed hydrogen decreased slightly. The reason for this decrease might be the deposition of a large amount of corrosion product on the surface of the specimens.

For α titanium, the side surfaces of a nonimmersed specimen and specimens immersed for 2000 and 10,000 h are shown in Figure 3(a–c), respectively. Similarly, for the α-β titanium, β titanium, and Ni-Ti superelastic alloys, the side surfaces of a nonimmersed specimen and specimens immersed for 2000 and 10,000 h are shown in Figures 4(a–c), 5(a–c), and 6(a–c), respectively. On the side surfaces of all specimens before immersion, scratches from SiC paper pol-

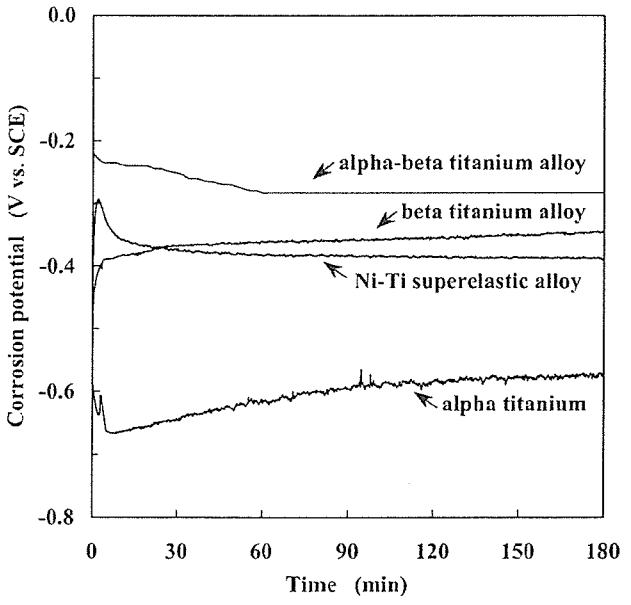

Figure 1. Changes in corrosion potentials of α titanium, α-β titanium, β titanium, and Ni-Ti superelastic alloys under aerated conditions in 2.0% NaF solution at 37°C.

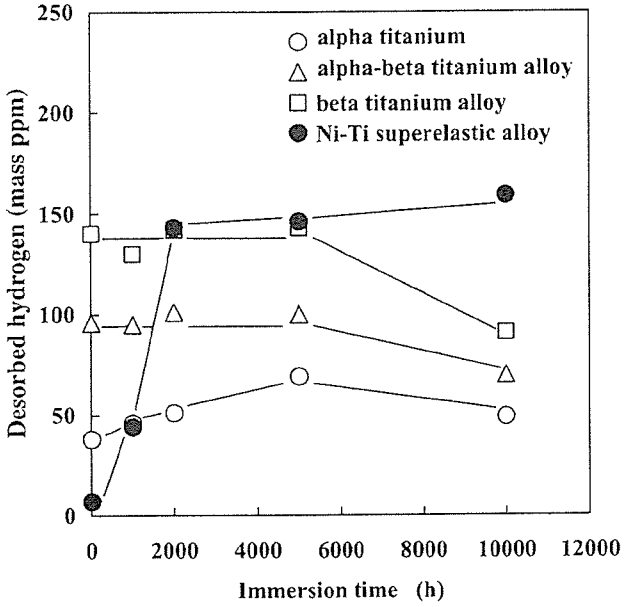

Figure 2. Amounts of hydrogen desorbed as functions of immersion time for α titanium, α-β titanium, β titanium, and Ni-Ti superelastic alloys immersed in 2.0% NaF solution.

ishing were observed. After immersion, the scratches on the surfaces of α titanium, and the α-β titanium and β titanium alloys partially disappeared due to general corrosion, while those on the surface of Ni-Ti superelastic alloy immersed up to 10,000 h remained. Corrosion products deposited on the surfaces of all immersed specimens, although the morphologies and amounts of corrosion products were not always the same. Only for α titanium did corrosion products tend to peel off the surface of the specimen.

Figure 7(a–h) shows the results of XRD measurements for the side surfaces of the nonimmersed specimens and specimens immersed for 2000 h. The presence of titanium hydride was confirmed on the surface of the immersed specimen of α titanium. Corrosion products on the surfaces of the immersed specimens of α titanium and the α-β titanium alloy were identified as Na_3TiF_6 and Na_3AlF_6, respectively. For immersed β titanium alloy, diffraction peaks related to corrosion products or hydrides were not detected irrespective of immersion time. In the case of Ni-Ti superelastic alloy, diffraction peaks except the parent phase (B2 structure) of Ni-Ti alloy were not identified because of the detection limit of the technique. Nevertheless, the small peak of ~39° for immersed Ni-Ti superelastic alloy disappeared, when the surface of the immersed specimen were carefully polished by SiC paper. Thus, this peak probably results from corrosion products and/or hydrides.

DISCUSSION

These results indicate that α titanium absorbs hydrogen in the neutral 2.0% NaF solution at 37°C during long-term immersion, thereby forming titanium hydride, which—despite its corrosion potential—is stable at −0.6 V (vs. SCE). Moreover, Ni-Ti superelastic alloy absorbs substantial amounts of hydrogen at a corrosion potential of −0.4 V (vs. SCE) in the 2.0% NaF solution. After 1000–2000 h, the effects of immersion time on hydrogen absorption and/or corrosion were small under these experimental conditions. On the other hand, the α-β titanium and β titanium alloys do not absorb sufficient amounts of hydrogen to lead to the degradation of mechanical properties. In most previous studies,[10–14] corrosion behavior of titanium or Ni-Ti alloys in fluoride solutions was examined for relatively short-term immersion. In the present study, the corrosion potential was stabilized for a few

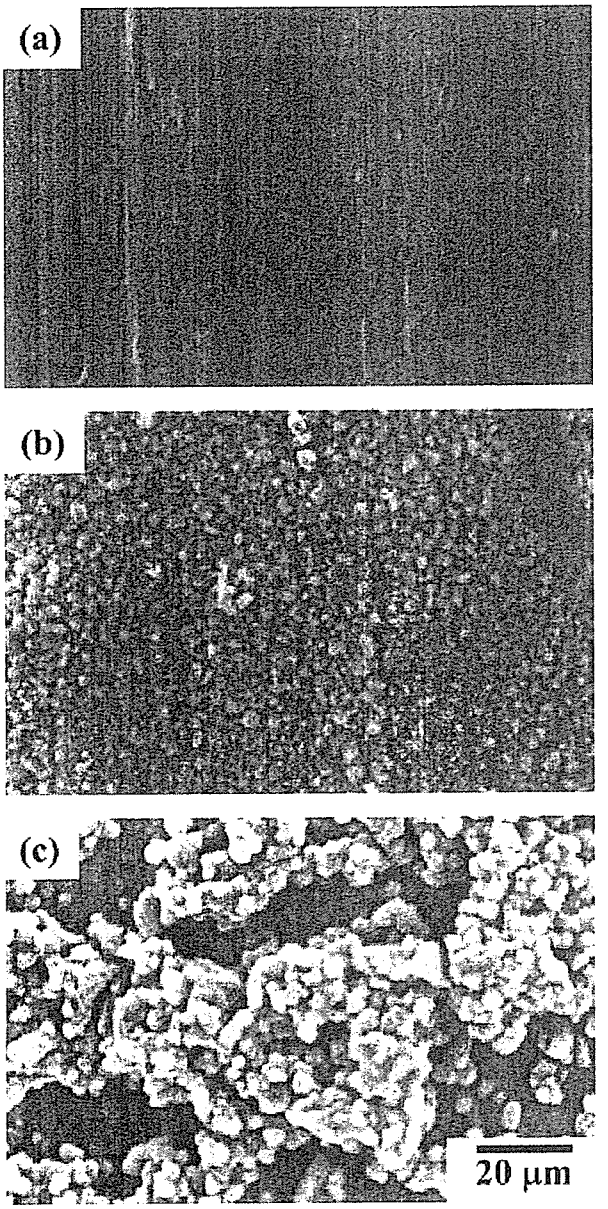

Figure 3. SEM images of typical side surface of α titanium. (a) Nonimmersed specimen and specimens immersed in 2.0% NaF solution for (b) 2000 h and (c) 10,000 h.

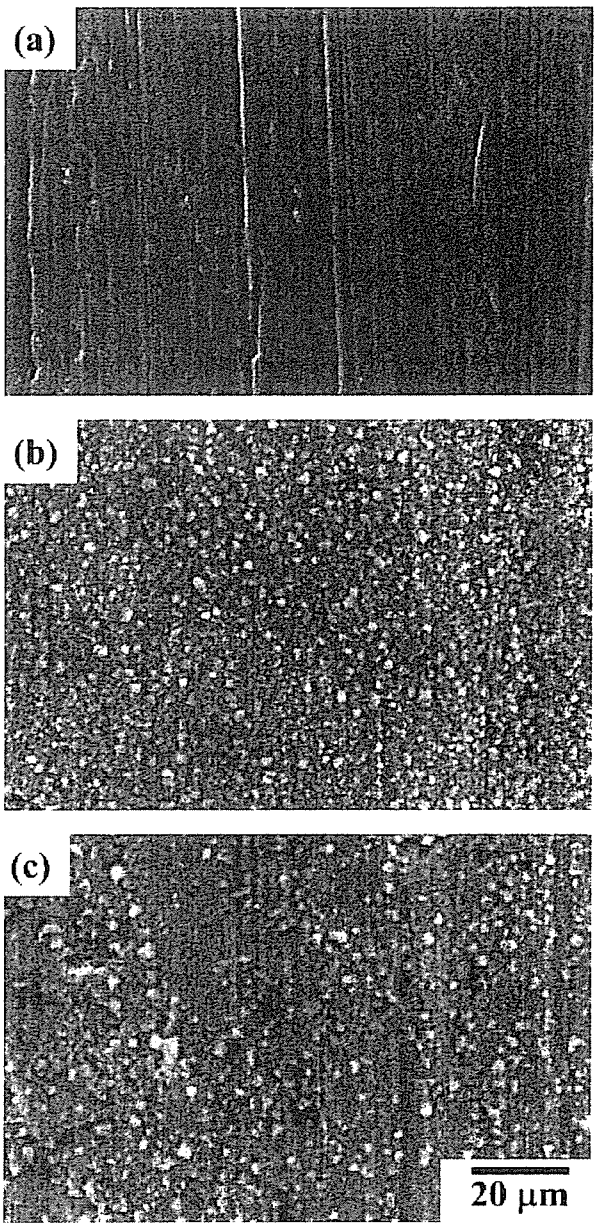

Figure 4. SEM images of typical side surface of α-β titanium alloy. (a) Nonimmersed specimen and specimens immersed in 2.0% NaF solution for (b) 2000 h and (c) 10,000 h.

hours as shown in Figure 1, but general corrosion was observed for long-term immersion (Figures 3–5). If the corrosion potential is measured for long-term immersion, it will be different from that measured for short-term immersion.

For α titanium, when the amount of absorbed hydrogen is larger than a few hundreds mass ppm, the mechanical properties markedly degrade in relation to brittle hydride formation.[15,16] As shown in Figure 7(b), hydride formation was confirmed for α titanium immersed in the 2.0% NaF solution. The amount of absorbed hydrogen obtained from TDA was at most 10–30 mass ppm (Figure 2), which was the average value over the entire specimen. The hydrogen content near the surface of a specimen is probably much higher than that at the center of the specimen, because hydride formation at several tens of micrometers from the surface of the specimen prevents hydrogen diffusion to the center of the specimen and serves as a barrier to further hydrogen absorption at 37°C.[17,18] Actually, in the case of α titanium immersed in the 2.0% acidulated phosphate fluoride (APF) solution,[19] the hydrogen content of the surface layer was evaluated as ~5000 mass ppm, although the average hydrogen content of the entire specimen was 900 mass ppm. Thus, even if hydrogen absorption is 10–30 mass ppm, hydrogen enrichment at the surface of the specimen probably allows the formation of a large quantity of hydride that can be detected by XRD

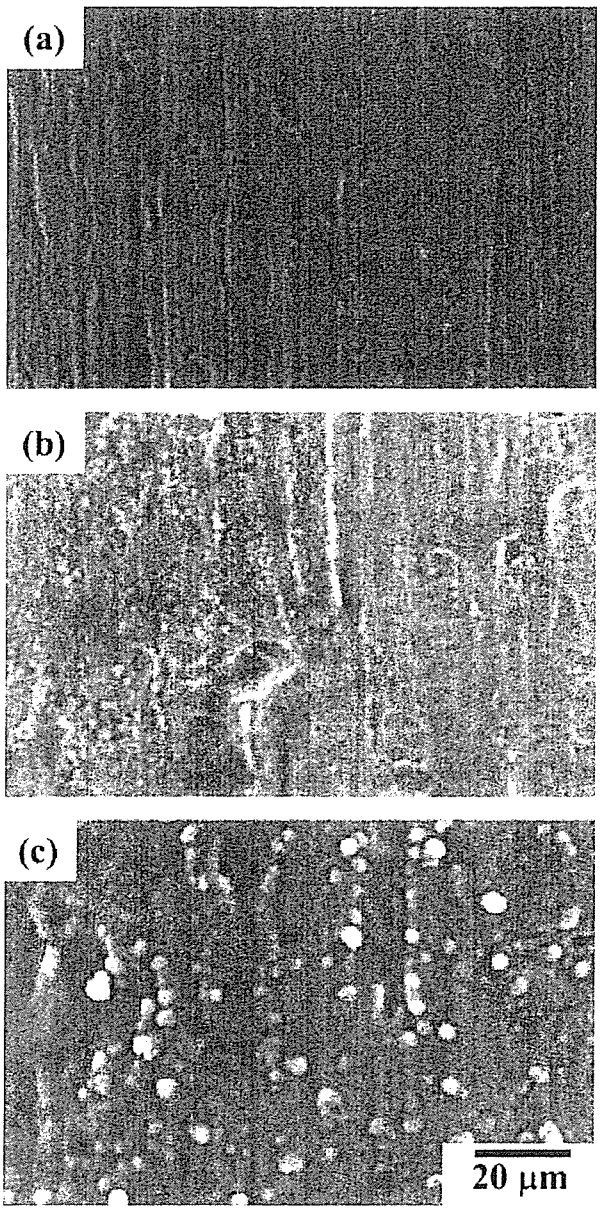

Figure 5. SEM images of typical side surface of β titanium alloy. (a) Nonimmersed specimen and specimens immersed in 2.0% NaF solution for (b) 2000 h and (c) 10,000 h.

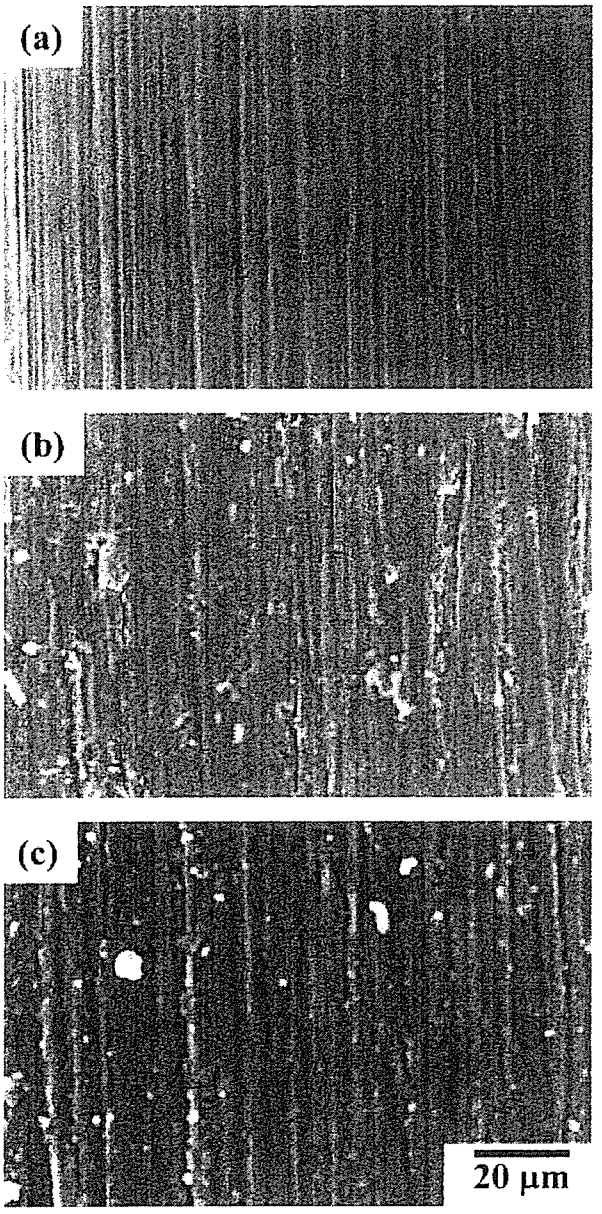

Figure 6. SEM images of typical side surface of Ni-Ti superelastic alloy. (a) Nonimmersed specimen and specimens immersed in 2.0% NaF solution for (b) 2000 h and (c) 10,000 h.

measurement. The surface layer containing hydride is brittle, peeling readily off the surface of the α titanium under applied stress. Consequently, it is likely that our previous result[3] regarding the fracture of α titanium under a sustained tensile-loading test in neutral 2.0% NaF solution is attributed to ductility loss in the surface layer associated with hydride formation and a reduction in the cross section of the specimen because of peeling of the surface.

For Ni-Ti superelastic alloy, the amount of hydrogen absorbed in 2.0% NaF solution (~150 mass ppm) is presumably sufficient to result in the pronounced degradation of mechanical properties. When the amount of absorbed hydrogen exceeds 50–200 mass ppm, ductility loss in the Ni-Ti superelastic alloy is often observed.[1,20,21] Since hydrogen absorption by the Ni-Ti superelastic alloy is markedly enhanced in the stress-induced martensite phase,[4,22] the amount of absorbed hydrogen under an applied stress above the critical stress for martensite transformation could become larger than that in this study. Under an applied stress higher than the critical stress for martensite transformation, however, fracture due to active path corrosion accompanied by hydrogen absorption occurs within 1000 h.[4] As for hydrogen absorption of Ni-Ti superelastic alloy in the 2.0% NaF solution, it should be emphasized that hydrogen absorption occurred despite the remaining scratches from SiC paper polishing, that is, very slight corrosion.

For both the α-β titanium and β titanium alloys, corrosion similar to that of α titanium was observed as shown in Figures 4 and 5, but the increments in the amounts of desorbed hydrogen and hydride formed were not confirmed. Generally, the hydride is rarely formed in many β titanium alloys[23,24] and is formed at a hydrogen content of more than 650 mass ppm in the α-β titanium alloy.[25] In this study, surface morphologies subjected to the immersion test without applied stress were different from those with applied stress that were reported previously.[2,7] Under a sustained tensile-loading test in 2.0% NaF solution lasting up to 1000 h, scratches from SiC paper polishing disappeared completely in association with corrosion enhanced by applied stress, and innumerable corrosion pits were observed on the surface of the specimens. Nonetheless, the α-β titanium and β titanium alloys subjected to an applied stress even around the yield stress did not fracture in 2.0% NaF solution.[2,7] Since the hydride does not form on the surface layer of either alloy, it is likely that the surface layer hardly peels off from the surface. In addition, the susceptibility to hydrogen embrittlement of the β titanium alloy is lower than that of α titanium in the case of the same hydrogen content, because the β titanium phase has a high solubility limit for hydrogen. Accordingly, we suggest for the present that the marked degradation of the mechanical properties of the α-β titanium and β titanium alloys caused by hydrogen absorption does not occur in neutral fluoride solutions, although in regard to corrosion additional study is warranted. Furthermore, relationships between corrosion and hydrogen absorption must be investigated for various titanium alloys in the future.

On the basis of our previous results from a sustained tensile-loading test in a 2.0% APF solution of pH 5.0, the susceptibility to hydrogen embrittlement of titanium alloys, that is, time-to-fracture under the same applied stress, is in the order of Ni-Ti superelastic alloy[4] > α titanium[3] and β titanium alloy[2] > α-β titanium alloy.[7] The time-to-fracture of the β titanium alloy is shorter than that of α titanium under an applied stress below 500 MPa. The hydrogen absorption rates of the Ni-Ti superelastic and β titanium alloys are one order of magnitude larger than those of the α titanium and the α-β titanium alloy in 2.0% APF solution. For instance, after immersion for 24 h in the 2.0% APF solution at 25°C, the amounts of hydrogen absorbed by the Ni-Ti superelastic alloy, the β titanium alloy,[5] α titanium[6] and the α-β titanium

DOI 10.1002/jbmb

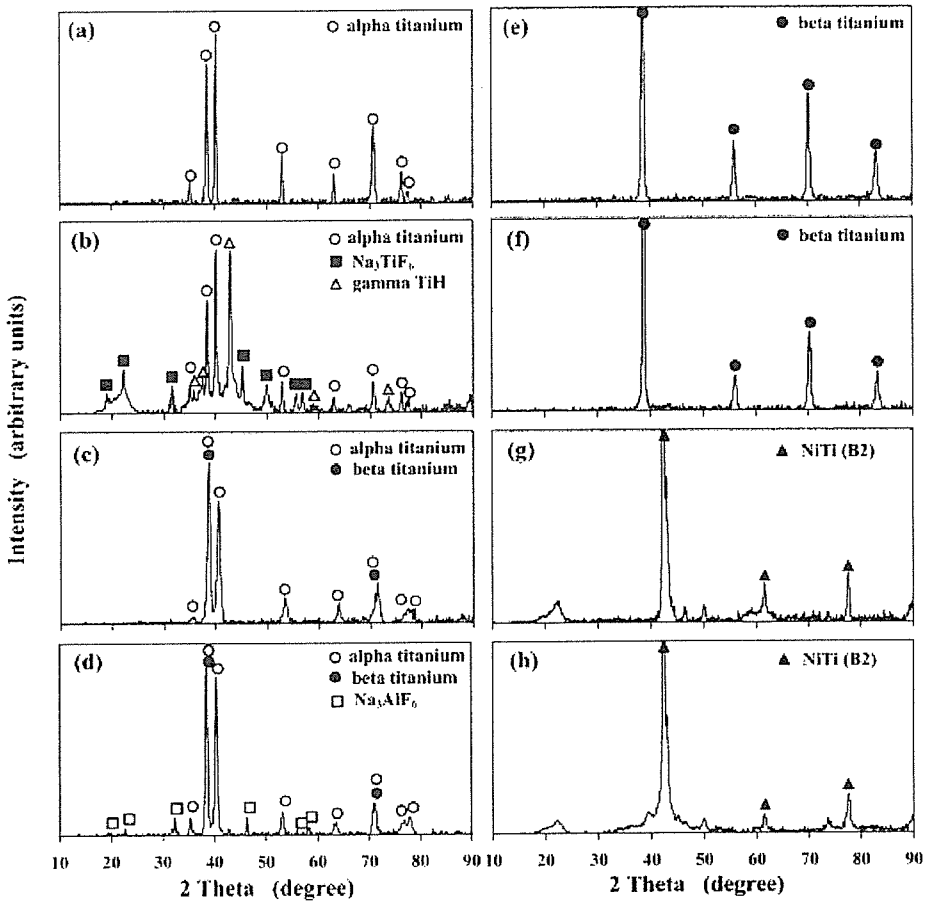

Figure 7. XRD patterns for surface of (a) nonimmersed α titanium, (b) α titanium immersed in 2.0% NaF solution for 2000 h, (c) nonimmersed α-β titanium alloy, (d) α-β titanium alloy immersed in 2.0% NaF solution for 2000 h, (e) nonimmersed β titanium alloy, (f) β titanium alloy immersed in 2.0% NaF solution for 2000 h, (g) nonimmersed Ni-Ti superelastic alloy, and (h) Ni-Ti superelastic alloy immersed in 2.0% NaF solution for 2000 h.

alloy[7] are approximately 1000, 4000, 200, and 200 mass ppm, respectively. The susceptibility to hydrogen absorption of titanium alloys in neutral 2.0% NaF solution is not always in agreement with that in 2.0% APF solution. This finding indicates that hydrogen absorption properties must be examined under various conditions.

CONCLUSIONS

We have demonstrated that α titanium and Ni-Ti superelastic alloy absorb hydrogen, which is probably sufficient to lead to the degradation of the mechanical properties in a neutral 2.0% NaF solution. In contrast, the α-β titanium and β titanium alloys hardly absorb hydrogen, even during long-term immersion, although general corrosion occurs. The susceptibility to hydrogen absorption of titanium alloys in neutral fluoride solution is not necessarily consistent with that in acidic fluoride solution.

REFERENCES

1. Yokoyama K, Kaneko K, Moriyama K, Asaoka K, Sakai J, Nagumo M. Hydrogen embrittlement of Ni-Ti superelastic alloy in fluoride solution. J Biomed Mater Res A 2003;65: 182–187.
2. Kaneko K, Yokoyama K, Moriyama K, Asaoka K, Sakai J, Nagumo M. Delayed fracture of β titanium orthodontic wire in fluoride aqueous solutions. Biomaterials 2003;24:2113–2120.
3. Yokoyama K, Kaneko K, Miyamoto Y, Asaoka K, Sakai J, Nagumo M. Fracture associated with hydrogen absorption of sustained tensile-loaded titanium in acid and neutral fluoride solutions. J Biomed Mater Res A 2004;68:150–158.
4. Yokoyama K, Kaneko K, Moriyama K, Asaoka K, Sakai J, Nagumo M. Delayed fracture of Ni-Ti superelastic alloys in acidic and neutral fluoride solutions. J Biomed Mater Res A 2004;69:105–113.
5. Ogawa T, Yokoyama K, Asaoka K, Sakai J. Hydrogen absorption behavior of β titanium alloy in acid fluoride solutions. Biomaterials 2004;25:2419–2425.
6. Yokoyama K, Ogawa T, Asaoka K, Sakai J. Hydrogen absorption of titanium in acidic fluoride solutions. Mater Sci Eng A 2004;384:19–25.

7. Yokoyama K, Ogawa T, Asaoka K, Sakai J. Susceptibility to delayed fracture of α-β titanium alloy in fluoride solutions. Corros Sci 2005;47:1778–1793.
8. Lausmaa J, Kasemo B, Hansson S. Accelerated oxide grown on titanium implants during autoclaving caused by fluorine contamination. Biomaterials 1985;6:23–27.
9. Könönen MHO, Lavonius ET, Kivilahti JK. SEM observations on stress corrosion cracking of commercially pure titanium in a topical fluoride solution. Dent Mater 1995;11:269–272.
10. Oda Y, Kawada E, Yoshinari M, Hasegawa K, Okabe T. The influence of fluoride concentration on the corrosion of titanium and titanium alloys. Jpn J Dent Mater Dev 1996;15:317–322.
11. Reclaru L, Meyer J-M. Effects of fluorides on titanium and other dental alloys in dentistry. Biomaterials 1998;19:85–92.
12. Nakagawa M, Matsuya S, Shiraishi T, Ohta M. Effect of fluoride concentration and pH on corrosion behavior of titanium for dental use. J Dent Res 1999;78:1568–1572.
13. Huang HH. Electrochemical impedance spectroscopy study of strained titanium in fluoride media. Elecrochim Acta 2002;47: 2311–2318.
14. Schiff N, Grosgogeat B, Lissac M, Dalard F. Influence of fluoride content and pH on the corrosion resistance of titanium and its alloys. Biomaterials 2002;23:1995–2002.
15. Lenning GA, Craighead CM, Jaffee RI. Constitution and mechanical properties of titanium-hydrogen alloys. Trans Metall Soc AIME 1954;200:367–376.
16. Williams DN. The hydrogen embrittlement of titanium alloys. J Inst Metals 1962;91:147–152.
17. Phillips II, Poole P, Shreir LL. Hydride formation during cathodic polarization of Ti. II. Effect of temperature and pH of solution on hydrogen growth. Corros Sci 1974;14:533–542.
18. Wang ZF, Briant CL, Kumar KS. Hydrogen embrittlement of grade 2 and grade 3 titanium in 6% sodium chloride solution. Corrosion 1998;54:553–560.
19. Ogawa T, Yokoyama K, Asaoka K, Sakai J. Distribution and thermal desorption behavior of hydrogen in titanium alloys immersed in acidic fluoride solutions. J Alloys Compd 2005; 396:269–274.
20. Yokoyama K, Ogawa T, Asaoka K, Sakai J, Nagumo M. Degradation of tensile strength of Ni-Ti superelastic alloy due to hydrogen absorption in methanol solution containing hydrochloric acid. Mater Sci Eng A 2003;360:153–159.
21. Ogawa T, Yokoyama K, Asaoka K, Sakai J. Hydrogen embrittlement of Ni-Ti superelastic alloy in ethanol solution containing hydrochloric acid. Mater Sci Eng A 2005;393:239–246.
22. Yokoyama K, Watabe S, Hamada K, Sakai J, Asaoka K, Nagumo M. Susceptibility to delayed fracture of Ni-Ti superelastic alloy. Mater Sci Eng A 2003;341:91–97.
23. McQuillan AD. An experimental and thermodynamic investigation of the hydrogen-titanium system. Proc R Soc London Ser A 1950;204:309–323.
24. Paton NE, Williams JC. Effect of hydrogen on titanium and its alloys. In: Bernstein IM, Thompson AW, editors. Hydrogen in Metals. Metals Park, OH: ASM; 1974. p 409–432.
25. Pittinato GF, Hanna WD. Hydrogen in β transformed Ti-6Al-4V. Metall Trans 1972;3:2905–2909.

ELSEVIER

Materials Science and Engineering A 422 (2006) 218–226

MATERIALS SCIENCE & ENGINEERING A

www.elsevier.com/locate/msea

Effects of moisture and dissolved oxygen in methanol and ethanol solutions containing hydrochloric acid on hydrogen absorption and desorption behaviors of Ni–Ti superelastic alloy

Toshio Ogawa [a], Ken'ichi Yokoyama [b,*], Kenzo Asaoka [b], Jun'ichi Sakai [a]

[a] *Department of Materials Science and Engineering, Waseda University, 3-4-1 Okubo, Shinjuku-ku, Tokyo 169-8555, Japan*
[b] *Department of Biomaterials and Bioengineering, Institute of Health Biosciences, The University of Tokushima Graduate School, 3-18-15 Kuramoto-cho, Tokushima 770-8504, Japan*

Received 15 November 2005; received in revised form 1 February 2006; accepted 3 February 2006

Abstract

The effects of moisture (H_2O concentration) and dissolved oxygen in methanol and ethanol solutions containing 0.1% hydrochloric acid (HCl) on hydrogen absorption and desorption behaviors of the Ni–Ti superelastic alloy have been examined by hydrogen thermal desorption analysis. In the methanol solution, the amount of absorbed hydrogen decreases with increasing H_2O concentration. For 5% H_2O, the thermal desorption peak of hydrogen gradually shifts from 400 to 250 °C with immersion time. When the H_2O concentration is higher than 10%, the hydrogen absorption is not observed. Under a deaerated condition, significant dissolution of the specimen due to corrosion is observed; however, the increment in the amount of desorbed hydrogen is not observed. In the ethanol solution, the critical H_2O concentration for hydrogen absorption is approximately 0.8%. For 2% H_2O, the hydrogen absorption is not exhibited, although slight corrosion is observed. The amount of absorbed hydrogen under the deaerated condition is ten times more than that under the aerated condition. The dissolved oxygen varies the hydrogen desorption behavior.

Keywords: Ni–Ti; Hydrogen embrittlement; Corrosion; Methanol solution; Ethanol solution

1. Introduction

We have recently found that the Ni–Ti superelastic alloy absorbs hydrogen through localized corrosion in methanol and ethanol solutions containing 0.1% hydrochloric acid (HCl), thereby causing hydrogen embrittlement [1,2]. Although the scattering of the amount of hydrogen absorbed in the methanol solution is relatively small [1], the occurrence of hydrogen absorption in the ethanol solution varies widely [2]. The origin of the scattering of hydrogen absorption has not been known, but the presence of moisture (H_2O concentration) and/or dissolved oxygen in the solutions is suspected because they affect sensitively the corrosion resistance of titanium and its alloys [3–7].

The presence of H_2O and dissolved oxygen in the methanol solutions produces an inhibiting effect to corrosion, improving the stability of the hydrated oxide film in the case of titanium and its alloys covered with a thin titanium oxide film [3–7]. Hence, it seems that the H_2O concentration and dissolved oxygen affect the hydrogen absorption behavior of the Ni–Ti superelastic alloy, because the surface of the Ni–Ti superelastic alloy is covered with mainly titanium oxide film.

In contrast, in the ethanol solution, no corrosion of titanium and its alloys occurs [3]. Moreover, no effects of H_2O concentration and dissolved oxygen on the stability of titanium oxide film in ethanol solution containing NaCl are observed, except changing of breakdown potential [5]. However, the Ni–Ti superelastic alloy undergoes localized corrosion in the ethanol solution [2]; the hydrogen absorption behavior of the alloy possibly depends on the H_2O concentration and dissolved oxygen. To understanding the hydrogen embrittlement characteristic of the Ni–Ti superelastic alloy in the methanol and ethanol solutions, it is necessary to investigate the effects of the H_2O concentration and dissolved oxygen on the hydrogen absorption behavior. In particular, the minimum critical H_2O concentration needed to

* Corresponding author. Tel.: +81 88 633 7334; fax: +81 88 633 9125.
E-mail address: yokken@dent.tokushima-u.ac.jp (K. Yokoyama).

0921-5093/$ – see front matter © 2006 Elsevier B.V. All rights reserved.
doi:10.1016/j.msea.2006.02.005

avoid hydrogen absorption is important from the standpoint of inhibiting hydrogen embrittlement.

Because the thermal desorption behavior of hydrogen reflects the state of hydrogen (e.g., hydride, trapped in a defect, in solution) or trap sites in the materials, the correlation of the responsible hydrogen for the embrittlement can be clarified [8–15]. The hydrogen desorption of the Ni–Ti superelastic alloy immersed in the methanol solution appeared as a desorption peak at 350–400 °C [1], whereas that in the ethanol solution appeared as two peaks at approximately 150 and 350 °C [2]. Relationships between the hydrogen desorption behavior and the degradation behavior of mechanical properties of the Ni–Ti superelastic alloy immersed in the methanol solution [1] are not always agreement with those in the ethanol solution [2]. In the present situation where the cause of the change of the hydrogen desorption behavior is not clear, it is difficult to predict and analyze the effects of the H_2O concentration and dissolved oxygen in the methanol and ethanol solutions on the hydrogen desorption behavior of the Ni–Ti superelastic alloy. Therefore, for the future analysis of the state of hydrogen or trap sites, the basic data of the hydrogen desorption behavior must be accumulated at the beginning.

The objective of the present study is to investigate effects of H_2O concentration and dissolved oxygen on hydrogen absorption and desorption behaviors of the Ni–Ti superelastic alloy in methanol and ethanol solutions containing 0.1% HCl by hydrogen thermal desorption analysis (TDA).

2. Experimental procedures

2.1. Materials

A commercial Ni–Ti (Ni: 55 mass%, Ti: balance) superelastic alloy wire 0.50 mm in diameter (described previously [2]) was cut into specimens 50 mm in length. Hereafter, percent in this paper means mass percent, unless otherwise stated. The specimens were polished with 600-grit SiC papers and ultrasonically cleaned with acetone for 5 min. The mechanical properties and phase transformation temperatures of the specimen are listed in Table 1, in which M_s and M_f are the start and finish temperatures for martensite transformation, respectively, on cooling. Similarly, A_s and A_f indicate the start and finish temperatures, respectively, for the reverse transformation on heating. The phase transformation temperatures of the specimen were determined by differential scanning calorimetry (DSC) at a scan rate of 10 °C/min. The critical stress for martensite transformation and the tensile strength were measured at room temperature (25 ± 2 °C). Standard deviation was calculated from the results obtained from five specimens.

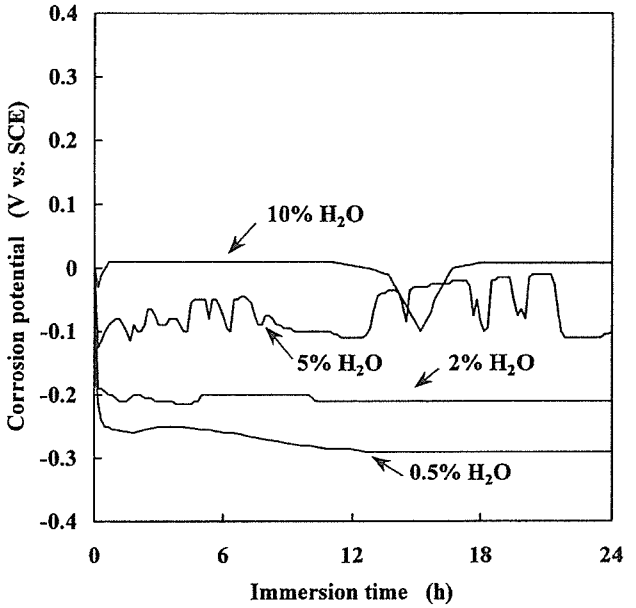

Fig. 1. Changes in corrosion potentials of Ni–Ti superelastic alloy specimens in 0.1% HCl-containing methanol solutions with various H_2O concentrations.

2.2. Test solutions

Chemical-agent-grade methanol or ethanol solutions containing 0.1 mass% HCl were used as the test solutions. These solutions contained initially 0.5 and 0.8 mass% H_2O, respectively. To examine the effects of H_2O, various H_2O concentrations of the test solutions were prepared by adding distilled water. The temperature of the test solutions was kept at 37 ± 0.5 °C.

2.3. Corrosion test

Corrosion potentials of the specimens were measured in 150 ml of the test solutions. The counter and reference electrodes used were a platinum electrode and a saturated calomel electrode (SCE), respectively. To determine the effects of dissolved oxygen concentrations, test solutions exposed to air and deaerated by 99.999% N_2 gas bubbling for 90 min with 190 ml/cm^2 solution were used. The measurements were started 10 s after immersion in the test solutions.

2.4. Immersion test

The specimens were immersed separately in 10 ml of the test solutions for various periods. The mass losses of the immersed specimens with immersion time were measured using a microbalance. The side surfaces of the nonimmersed

Table 1
Mechanical properties and transformation temperatures of tested Ni–Ti superelastic alloy

Critical stress (MPa)	Tensile strength (MPa)	Reduction in area (%)	Transformation temperature (°C)			
			A_f	A_s	M_s	M_f
535 ± 1.4	1425 ± 12.6	54.6	7.5	−26.0	2.5	−38.5

and immersed specimens were observed by scanning electron microscopy (SEM).

2.5. Thermal desorption analysis

The present experimental conditions of TDA were the same as those of our previous studies [1,2]. The amount of desorbed hydrogen was measured by TDA with the specimens subjected to immersion or corrosion tests. Both ends of each specimen (50 mm in length) immersed in the test solution were cut into 20-mm-long segment and subjected to ultrasonic cleaning with acetone for 2 min. The segment was dried in ambient air and used for measurement. TDA was carried out 30 min after the removal of the specimen from the test solution. A quadrupole mass spectrometer (ULVAC, Kanagawa, Japan) was used for the detection of hydrogen. Data sampling was conducted at 30-s intervals at a heating rate of 100 °C/h. The amount of desorbed hydrogen was defined as the integrated peak intensity.

3. Results and discussion

3.1. Effects of H_2O concentration in methanol solution

Fig. 1 shows the effects of the H_2O concentration in methanol solution with 0.1% HCl on the corrosion potential of the Ni–Ti superelastic alloy under the aerated condition. For 0.5% H_2O,

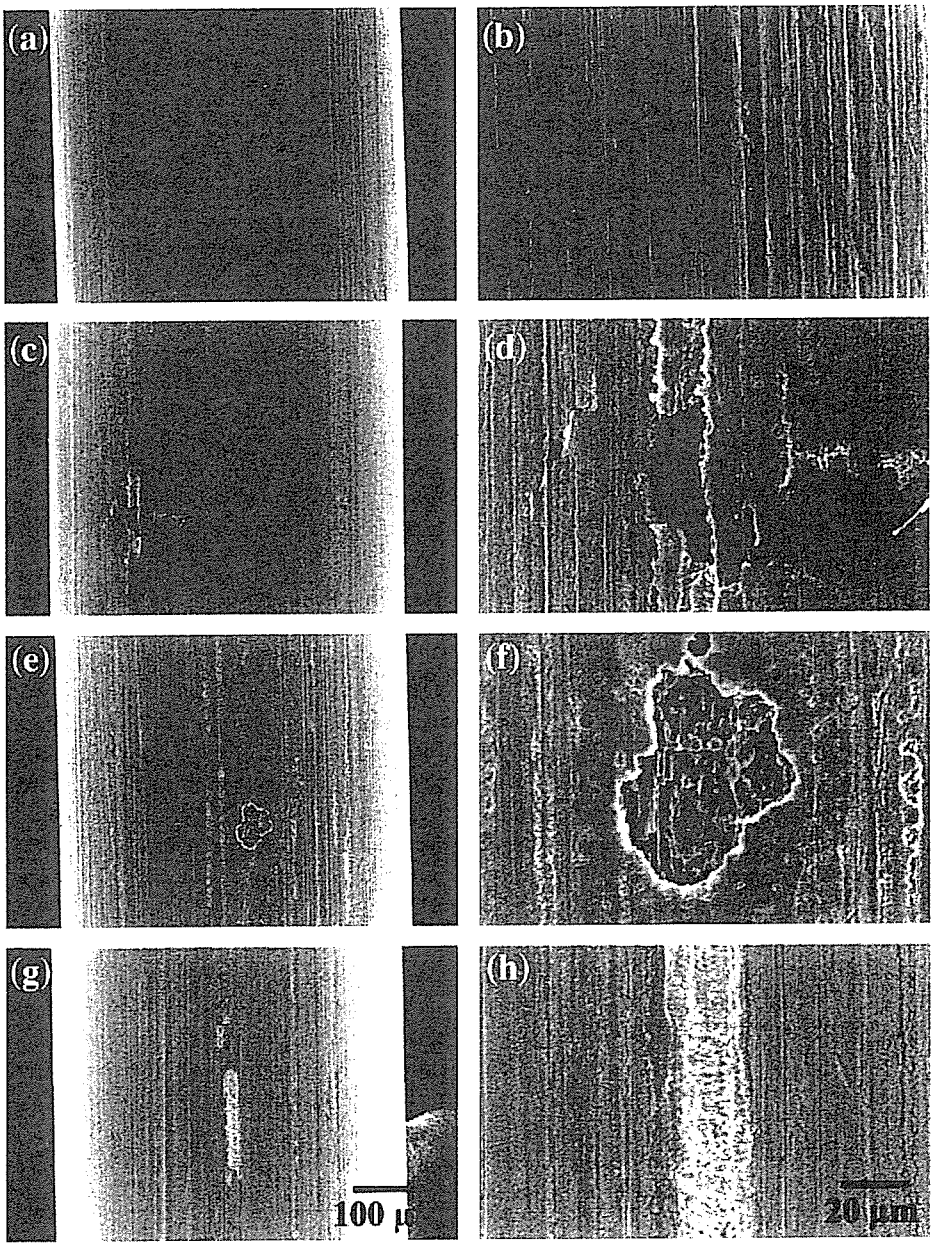

Fig. 2. SEM images of typical side surface: (a) general and (b) magnified views of nonimmersed specimen; (c) general and (d) magnified views of specimen immersed in methanol solution with 2% H_2O for 120 h; (e) general and (f) magnified views of specimen immersed in methanol solution with 5% H_2O for 120 h; and (g) general and (h) magnified views of specimen immersed in methanol solution with 10% H_2O for 120 h.

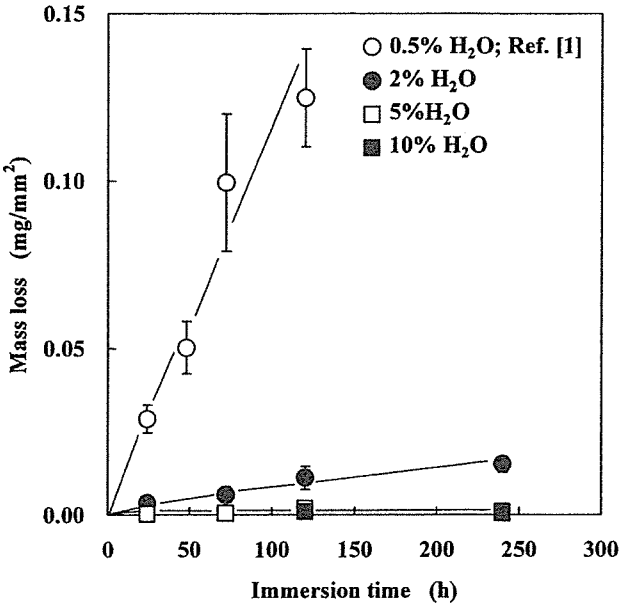

Fig. 3. Mass losses of specimens immersed in methanol solutions with various H_2O concentrations. Standard deviation was calculated from the results of five specimens.

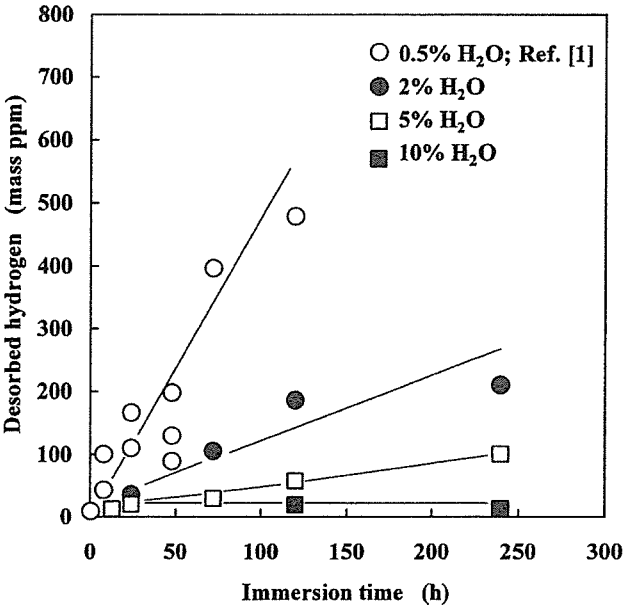

Fig. 4. Amounts of desorbed hydrogen obtained from thermal desorption analysis of specimens immersed in methanol solutions with various H_2O concentrations.

the corrosion potential shifted to the less noble direction immediately after immersion, and then it stabilized at −0.3 V. The corrosion potentials located in the noble direction with increasing H_2O concentration in the methanol solution.

On the side surface of the nonimmersed specimen, scratches due to SiC paper polishing were observed, as shown in Fig. 2(a) and (b). In our previous study [1], a large number of corrosion pits were observed on the surface of the specimen immersed in the methanol solution with 0.5% H_2O. Similarly, localized corrosion was observed for methanol solutions with 2%, 5% and 10% H_2O, as shown in Fig. 2(c)–(h). Corrosion area decreased with increasing H_2O concentration in the methanol solution.

As shown in Fig. 3, the mass losses of the specimens immersed in the methanol solution with 0.5% [1] and 2% H_2O increased with immersion time. The mass loss of the specimen immersed in the methanol solution with 0.5% H_2O was approximately 10 times that with 2% H_2O. When the H_2O concentration in the methanol solution was higher than 5%, the mass loss of the specimen was only slightly detected. These results show that the inhibiting effects of H_2O on the corrosion of the Ni–Ti superelastic alloy are similar to that of titanium and its alloys [3–7] in the methanol solutions. The reason for this is that the titanium hydroxide perhaps forms on the surface of the Ni–Ti superelastic alloy as well as on those of titanium and its alloys, as reported previously [4].

The amounts of desorbed hydrogen of specimens immersed in 0.1% HCl-containing methanol solutions with various H_2O concentrations are shown in Fig. 4. The amount of hydrogen absorbed during the immersion test can be calculated by subtracting the amount of hydrogen desorbed from a nonimmersed specimen, i.e., predissolved hydrogen content of 7 mass ppm, from the total amount of desorbed hydrogen. The amount of absorbed hydrogen increased with immersion time and decreased with increasing H_2O concentration in the methanol solution. For example, upon immersion in the methanol solution with 0.5%, 2% and 5% H_2O for 120 h, the amounts of absorbed hydrogen were approximately 500 [1], 200 and 60 mass ppm, respectively. In the methanol solution with 10% H_2O, the increment in the amount of desorbed hydrogen was not observed irrespective of immersion time. In the case of commercial pure titanium immersed in methanol solution containing 0.4% HCl, an addition of 1.5% H_2O is sufficient to inhibit stress corrosion cracking associated with hydrogen absorption [3,6,16–18]. It is likely that the effects of the H_2O concentration on corrosion and hydrogen absorption prevention in the methanol solution for the Ni–Ti superelastic alloy are one order of magnitude smaller than those for titanium. From Fig. 1, it appears that when the corrosion potential is less noble than approximately −0.1 V, the Ni–Ti superelastic alloy absorbs hydrogen in the methanol solution.

Hydrogen thermal desorption curves from specimens immersed in the 0.1% HCl-containing methanol solution with 2% H_2O are shown in Fig. 5(a). The primary desorption peak appeared at approximately 350 °C and a small secondary peak was observed at approximately 200 °C for an immersion time longer than 72 h. This hydrogen desorption behavior was analogous to that for specimens immersed in the 0.1% HCl-containing methanol solution with 0.5% H_2O, as reported previously [1]. In immersion in the methanol solution with 5% H_2O (Fig. 5(b)), the desorption peak shifted to lower temperature after 120 h, and appeared at approximately 250 °C for the specimen immersed for 240 h.

These results indicate that the H_2O concentration in the methanol solution sometimes affects the hydrogen desorption behavior. The hydrogen desorption behavior provides knowledge regarding the state of hydrogen or trap sites from the desorption profile and the amount of desorption. However, the

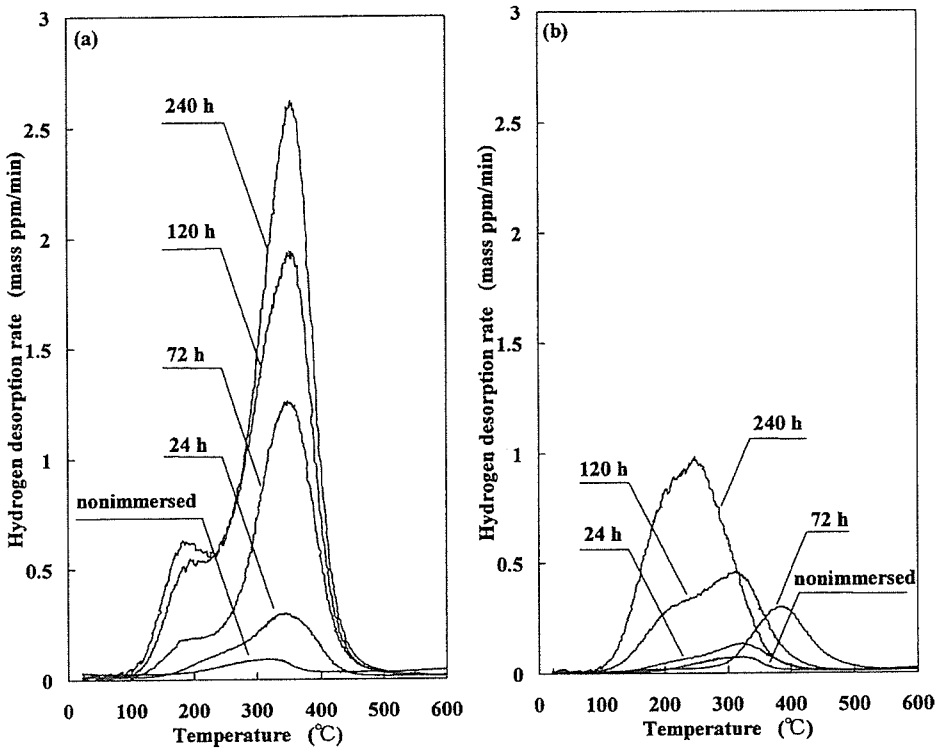

Fig. 5. Hydrogen thermal desorption curves obtained from specimens immersed for various periods in methanol solutions with (a) 2% H_2O and (b) 5% H_2O.

analysis must be performed carefully, because the hydrogen desorption behavior is sometimes influenced by various factors. For example, corrosion products on the surface of the beta titanium alloy often obstruct hydrogen desorption, thereby causing the desorption shift to high temperature [19]. In a separate experiment, we have confirmed that the hydrogen desorption behavior of the Ni–Ti superelastic alloy does not change when the surface of the specimen immersed in the methanol solution is slightly ground using SiC paper. Thus, effects of surface conditions of the specimen on the hydrogen desorption behavior can be neglected in the present study. Moreover, for the Ni–Ti superelastic alloy, the condition of hydrogen absorption often dominates whether hydrides form or not [20–25]. In the present study, hydride formation was not detected by X-ray diffraction (XRD) measurements; most of the absorbed hydrogen probably exists as trapped and/or in solution. Consequently, the change of the hydrogen desorption behavior may be attributed to the change of the state of hydrogen or trap sites, although unknown factors are excluded from the consideration.

3.2. *Effects of dissolved oxygen in methanol solution*

Fig. 6 shows the corrosion potential of the Ni–Ti superelastic alloy in 0.1% HCl-containing methanol solution with 0.5% H_2O under aerated and deaerated conditions. The potential under the deaerated condition was stabilized at −0.35 V and located in the less noble direction compared with that under the aerated condition.

General corrosion and corrosion products were revealed on the surface of the specimen immersed in the methanol solution for 24 h under the deaerated condition (Fig. 7(a) and (b)), whereas localized corrosion occurred under the aerated condition reported previously [1]. Under the deaerated condition, the diameter of the specimen was reduced from 0.50 to 0.38 mm.

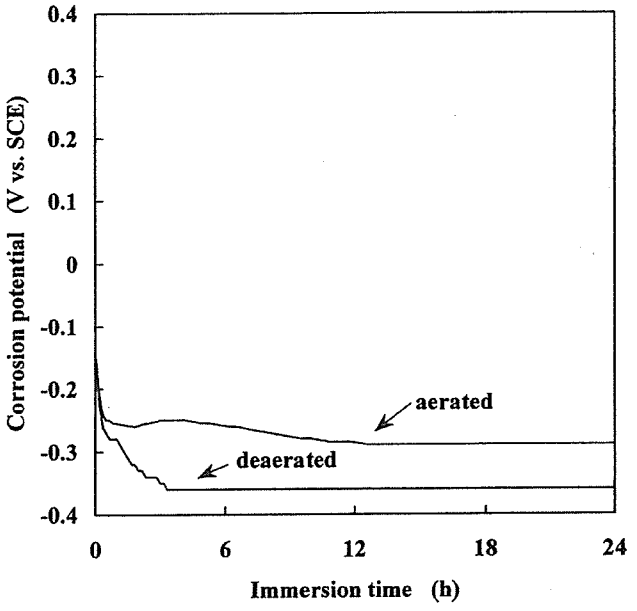

Fig. 6. Changes in corrosion potentials of specimen in methanol solution under aerated and deaerated conditions.

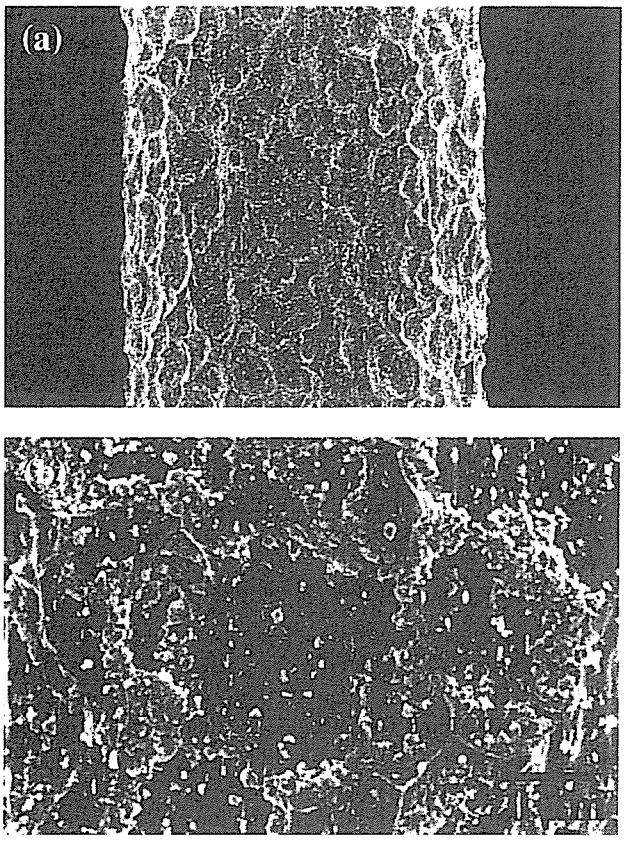

Fig. 7. SEM images of typical side surface of specimen immersed in methanol solution for 24 h under deaerated condition. (a) General and (b) magnified views.

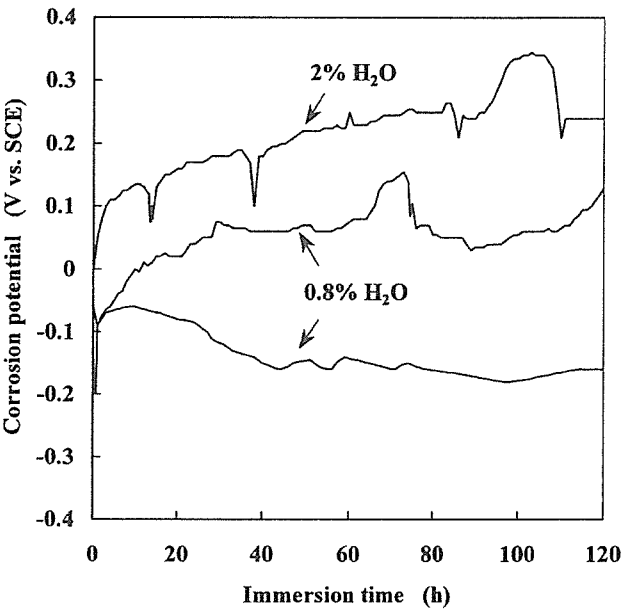

Fig. 8. Changes in corrosion potentials of specimens in ethanol solution with 0.8% and 2% H_2O.

This result indicates that the absence of dissolved oxygen leads to a steep increment in corrosion rate. Conversely, only a slight increment in the amount of desorbed hydrogen was confirmed for the immersed specimen under the deaerated condition. The probable reason for this is that the rate of dissolution due to corrosion of the surface layer of the immersed specimen was larger than the diffusion rate of hydrogen. The diffusion distance of hydrogen in the specimen is calculated to be approximately 50 μm at most for 24 h at 37 °C, using the diffusion coefficient of hydrogen in Ni–Ti alloy with a B2 structure reported by Schmidt et al. [26].

3.3. Effects of H_2O concentration in ethanol solution

Fig. 8 shows the changes in the corrosion potentials of the Ni–Ti superelastic alloy in the 0.1% HCl-containing ethanol solution with 0.8% and 2% H_2O under the aerated condition. For 0.8% H_2O, the corrosion potential varied widely and was classified into two behaviors. One corresponds to the corrosion potential ranging from −0.1 to −0.2 V. In this case, the hydrogen absorption was observed; the hydrogen thermal desorption behavior and the side surface of the immersed specimen subjected to corrosion have been reported in our previous article [2]. The other corresponds to the corrosion potential between −0.1 and 0.1 V. Only a weak hydrogen absorption was confirmed in this potential range. The critical corrosion potential for hydrogen

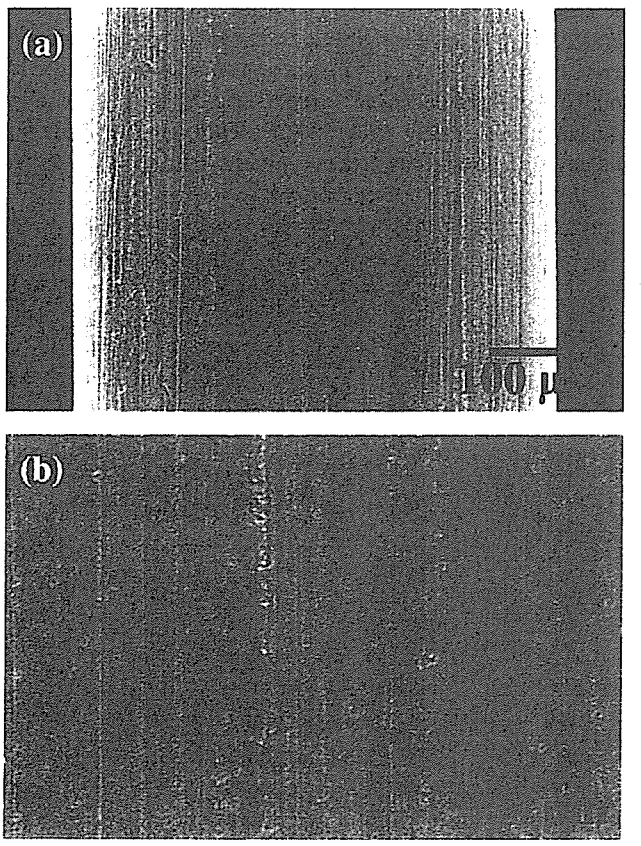

Fig. 9. SEM images of typical side surface of specimen immersed in ethanol solution with 2% H_2O for 120 h. (a) General and (b) magnified views.